Elongated Mitochondria Constrictions and fission in muscle fatigue

[1,2]Manuela Lavorato, [3]Emanuele Loro [4]Valentina Debattisti, [3]Tejvir Khurana, [1]Clara Franzini-Armstrong

[1]Dept. of Cell and Developmental Biology, University of Pennsylvania, Philadelphia, PA 19104
[2]Dept. of Genetics, Children's Hospital of Philadelphia, PA 19104
[3]Dept. of Physiology, University of Pennsylvania, Philadelphia, PA 19104
[4]MitoCare Center, Department of Pathology, Anatomy, and Cell Biology, Thomas Jefferson University, Philadelphia, PA 19107

Correspondence to: manuelalavorato@gmail.com

Key words: fatigue, fission, mitochondria, skeletal muscle.

Summary Statement

Exercise and electrical muscle stimulation increase the frequency of Elongated Mitochondria Constrictions (EMCs), a novel structural evidence for mitochondria dynamics stages in mice fast fibers.

Abstract

Mitochondria respond to stress and undergo fusion and fission at variable rates, depending on the cell status. To understand mitochondria behavior during muscle fatigue, we investigated mitochondria ultrastructure and the level of a fission and stress-related protein in fast muscle fibers of mice subjected to fatigue. Mice were forced running at increasing speed till exhaustion at 45'-1 hr. In other mice high-intensity muscle stimulation through the sciatic nerve simulated the forced treadmill exercise. We detect the unusual presence of a rare phenotype characterized by Elongated Mitochondria Constrictions (EMCs) connecting two separate segments of the original organelles. EMCs are rare in resting muscles and their frequency increases, albeit still at low levels, in stimulated muscles. The constrictions are accompanied by higher Drp-1 phosphorylation at Ser616, indicating an increased translocation of Drp-1 to mitochondria membrane. This is indicative of a mitochondrial stress response perhaps leading to or facilitating a long lasting fission event. A close apposition of

JCS Advance Online Article. Posted on 7 November 2018

SR to the constricted areas, detected by both transmission and scanning electron microscopy is highly suggestive of an SR involvement in inducing constrictions.

Introduction

Mitochondria, the cells' permanent guests, are very dynamic and extremely sensitive to their environment. They mostly have specific intracellular distributions that can directly contribute to the control of calcium homeostasis within the differentiated cells. (Tinel et al, 1999) and their precise positioning is at least in part due to small tethers that insure the association of the organelles with elements of the endoplasmic reticulum (Mannella et al, 1998) and of the sarcoplasmic reticulum (SR) in muscle (Boncompagni et al, 2009b). Mitochondrial fission and fusion events, obviously quite important during and immediately after cell division, are also continually occurring in interphase cells and are of primary importance in maintaining mitochondria size and shape as swell as, indirectly, cellular homeostasis and general heath of the individual (Chen and Chan, 2010; Westermann, 2010; Chan, 2012; Rana et al., 2017).

Mitochondria are extremely sensitive to the cytoplasmic milieu: they are directly affected by concentration changes of various cytoplasmic components, resulting in variations of their density, positioning, and ultrastructure. Structural mitochondria modulations are easily induced in muscle: for example, even an acute exercise of short duration may affect specific inter-mitochondria connections modulated by their surface membrane (Picard et al., 2013) and fragmentation can be induced by cardiac exercise (Coronado et al., 2018). Long-range effects occur in myopathies affecting calcium homeostasis, such as Central Core Disease and Malignant Hyperthermia in which mitochondria morphology, distribution and fragmentation are strongly affected (Boncompagni et al., 2009b; Lavorato et al., 2016). Prolonged unbalanced Ca^{2+} homeostasis in myocardium activates the fission process, resulting in increased frequency of mitochondria profiles due to fragmentation, while also inducing prolonged nanotunneling extensions in the usually structurally conservative cardiac mitochondria (Lavorato et al., 2015, 2017).

Striated muscles (skeletal and cardiac) are particularly appropriate subjects for the detection of subtle alterations in mitochondria ultrastructure, positioning and frequency, because the organelles have a highly stereotyped, developmentally regulated, cell type specific distribution in relationship to other cell components (Boncompagni et al., 2009a). Additionally, controlled alterations in cytoplasmic composition can be easily induced by subjecting the muscles to exercise and monitoring the induced fatigue. The term fatigue is generally used to indicate a complex alteration in muscle status in which the contraction response to a given stimulus is reduced in strength: it is not an absolute term, it involves intermediate stages in which muscle can still operate although at reduced power output levels, as well as terminal stages where no force is produced. Fatigue is due to a combination of causes mostly at the level of the muscle fiber itself even in experimental *in vivo* setups that involve contributions from respiratory and cardiovascular systems, nerve conduction and synaptic transmission (Fitt, 1994). Fatigue is a complex phenomenon, involving profound alterations in the cytoplasmic milieu (extensively reviewed by Fitt, 1994). For example, despite the cell's complex metabolic system that has evolved in order to insure basically constant ATP levels, loss of ATP, accumulation of ADP and general acidification of the cytoplasm accompany fatigue-inducing exercise (Westerblad and Allen, 1992, 1993). Additionally, changes in Mg levels, (Westerblad and Allen 1992b; Nassar-Gentina et al., 1981), accumulation of lactate from glycolysis and of inorganic phosphate from breakdown of creatine phosphate (Allen and Westerblad, 2001) and in more extreme cases changes in the rate of ATP hydrolysis (Nagasser et al., 1992) and reduction or failure to release calcium (Westerbad et al., 1993) can occur. Production and accumulation of active oxygen species has been more recently added to the list of fatigue related alterations (Cheng et al., 2016; Kamandulis et al., 2017). Oxygen demand is also altered during strong exercise: it may increase more than 20-fold in human skeletal muscle during intense exercise (Bangsbo et al., 2000).

The aim of this study was to detect ultrastructural alterations in mitochondria resulting from exercise and/or direct electrical stimulation that induced some level of fatigue. Fatigue

was detected by faltering in treadmill-exercised mice and by a reduction in recorded force response in electrically stimulated muscles. Both indicated an alteration in the cytoplasmic milieu that was likely to affect mitochondria. In order to see the accelerated effect of the stimulation we focused our analysis on the fibers most prone to fatigue: the fast, type IIB/IIX fibers. We discovered a novel structural modification of mitochondria with the appearance of elongated constrictions closely associated with SR elements. These may be indicative of a stress response and possibly of initial fission stages. The imaging was facilitated by the highly organized disposition of mitochondria in mouse skeletal muscle, which is rich in organized mitochondrial networks with complex interconnections (Franzini-Armstrong, 2007; Franzini-Armstrong and Boncompagni, 2011, Dahl et al., 2015; Glancy et al., 2015). In confirmation of the structural data we detected a fatigue related increase in the phosphorylation of Drp-1 at Ser616, a change that has been related to the translocation of Drp-1 to mitochondria membrane indicating a stress response of the mitochondria (Wei et al., 2011; Zhang et al., 2017) and possibly lead to the fission process (Taguchi et al., 2007).

Material and Methods

Experimental Animals. All animal experiments were in accordance with protocols approved by the Institutional Animal Care and Use Committee (IACUC) of Thomas Jefferson University and University of Pennsylvania. For treadmill experiments, 7-8 months old C57BL/6 mice were maintained at the Animal Core Facility of the Department of Pathology-Anatomy and Cell Biology, Thomas Jefferson University, accredited by AAALAC. For *in vivo* muscle stimulation, 5-6 month old C57BL/6 mice were used. Mice were housed at 22 °C under a 12-hour light/12-hour dark cycle with food and water provided ad libitum.

Treadmill exercise. 7-8 months old C5BL/6 mice were forced to exercise on a treadmill equipped with an electrical shock grid. Mice were previously acclimated for one week with a single 30 minutes run per day, with gradual increase of velocity up to 20m/min. For the test, mice were subjected to runs starting at a speed 10m/min, increasing by 2 m/min every 2 minutes up to a maximum of 20m/min. No mouse responded to repeated prodding at the end

of one hour running exercise on the treadmill, with some mice stopping to respond after 45 minutes. Mice that faltered before the 45 minutes period were not included in the subsequent analysis. Euthanasia by cervical dislocation was immediate at the end of the exercise and Extensor Digitorum Longus (EDL) muscles were harvested within minutes and processed for electron microscopy (EM) and for immunoblot analysis. Resting mice were used as controls.

Simulation of high-intensity exercise using electrical muscle stimulation. An *in vivo* sciatic nerve muscle stimulation protocol was developed in order to simulate the forced exercise of mice on treadmill. One leg of each mouse was stimulated, while the other leg was used as unstimulated control. Mice were anesthetized with 1-2% of isoflurane. Depth of anesthesia was confirmed by toe pinch and by monitoring the heart rate with a pulse oximeter. The sciatic nerve was exposed and connected to a custom made bipolar stimulating electrode driven by a Grass S48 stimulator. Two recording silver EMG needle electrodes were applied, one in the gastrocnemius and the other near the Achilles tendon. The ground electrode was connected to the skin of the back of the mouse. The recording electrodes were then connected to a Warner Instruments DP-311 differential amplifier and finally to an A/D converter. One leg of each mouse was electrically stimulated, the other acted as control. The EMG signal was used as a measure of fatigue. Muscles were collected immediately at the end of the stimulation: EDL was used for EM and Tibialis Anterior (TA) for western blot. Both muscles have a high content of fast fibers.

To design the stimulation protocol mice running on the treadmill at 20m/min were video recorded in order to visualize the stepping frequency. A back foot stepping frequency of 6Hz was observed, consistent with fast limb movements recorded in freely running mice (Bellardita and Kiehen, 2015). We designed a stimulation protocol that would subject the hind leg muscles to an exercise load equivalent to treadmill running. First, we observed that during 30 minutes experiments the mice run intermittently with short periods of inactivity. Based on this behavior, our maximal protocol consisted of stimulation bursts lasting 10 seconds, followed by 10 seconds of inactivity. This 10 sec on burst-10 sec off protocol lasted 30 minutes (Fig. 1). Secondly, we matched the stimulation pattern to that of fast running

posterior leg. Each 10s burst consisted of trains of 5Volt stimuli each lasting 0.1 sec at a frequency of 100 Hz, the normal frequency of fast fibers recorded *in vivo* (Hennig and Lomo, 1985) (Fig. 1C). Each train was repeated at the same frequency as the stepping (6Hz), with short intervals between, mimicking the pushing and retreating pattern of the hind foot. (Fig. 1B). Evoked action potentials were recorded through the stimulation. The high-intensity stimulation caused an 80% decrease in EMG amplitude within the first five minutes and a decline at each stimulus (Fig. 1A, B) possibly related to depletion of glycogen and phospho-creatine (Katz et al., 2003). Response decline within the following 25 minutes of stimulation was minor. The stimulation protocol induced the phosphorylation of known exercise-sensitive proteins such as p70/85S6K, AMPK, ERK (Potts et al., 2017; Hoffman et al., 2015) compared to non-stimulated sham control animal (sham -), non-stimulated sham control animal after 30 minutes (sham +), and the contralateral non-stimulated leg of the same animal (stim -) (Fig. 1 F).

Thin section electron microscopy (TEM). EDL muscles were dissected, pinned down at approximately resting length, fixed by immersion in 6% (vol/vol) glutaraldehyde in 0.1 M sodium cacodylate buffer (pH 7.4) at room temperature and further processed for standard TEM as in Lavorato et al. (2017). The embedded muscles were carefully mounted, so precisely oriented cross and longitudinal sections were routinely obtained (see supplementary Fig. S1).

TEM quantification. Electron microscopy and subsequent analysis were performed on cross sections of muscles. Observations were limited to fast fatigable fibers type IIB and IIX. Mouse EDL contains approximately 70-75% type IIB, 10—15% IIX, 8% IIA and 4% I (Hughes et al., 1999; Danielli-Betto et al., 2005). Type IIB and IIX fibers are easily distinguishable from the others by the fact that mitochondria are limited to the I bands and that clusters at the fibers' edges are not present. However, distinction between IIX and IIB is not obvious and so it was not attempted (Boncompagni et al., 2010). Mitochondria width was measured at several points along each profile in randomly selected EM images from muscle cross sections at a magnification of 26,300x using Fiji program (NIH). The frequency of

mitochondria showing elongated constrictions was very low, so quantitation required large sample sizes. We obtained very well oriented cross sections of large muscle bundles, each showing up to 50 fiber profiles. All IIX/IIB fiber profiles that appeared entirely in the section, not hindered by the thin grid bars were accepted for counting (see supplemental Fig. 1). Since the fast fibers are fairly uniform in diameter, the cross section areas was used as a reference. Elongated constrictions were visually identified and their numbers counted in each fiber cross section. The numbers, expressed as number of profiles/fiber cross section are proportional to the constriction frequencies in the fiber volume.

Scanning Electron microscopy. EDL muscles were fixed in 0.5% paraformaldehyde-1.0% glutaraldehyde at room temperature for a minimum of ½ hr; cryoprotected in 40% glycerol, frozen in propane; cryofractured and macerated by prolonged exposure to low concentration (~ 0.1%) of OsO4 for 48-72 hrs; critical point dried; sputter coated for conductivity and observed using FEI Quanta 250 SEM. The technique was developed by Tanaka and Mitsushima (1984) and effectively used by Ogata and Araki (1990), see also Ogata and Yamasaki (1993) for a review.

Western Blot analysis. EDL and TA muscles were homogenized and subjected to SDS-PAGE followed by immunoblot analysis, as previously described (Loro et al., 2015). All antibodies were purchased from Cell Signaling, except for α tubulin from Sigma-Aldrich (Phospho p70/85 S6 Kinase, Cell Signaling Technologies, clone 1A5, 1:2000; p70 S6 Kinase, Cell Signaling Technologies, clone 49D7, 1:2000; phospho AMPK T172, Cell Signaling Technologies, clone 40H9, 1:2000; AMPK, Cell Signaling Technologies, clone D5A2, 1:2000; Active MAPK (P-ERK1/2) - Promega, 1:5000; DRP1, BD Biosciences, clone 8/DRP1, 1:1000; Phospho DRP1 S616, Cell Signaling, 1:2000; tubulin, Sigma, T6199, 1:5000). Digital images of the plots were scanned using Fiji program (Imagej, NIH) to obtain pixel density of bands. The total pixel density for each band was used for the purpose of comparing protein amounts.

Results

Average mitochondria width is reduced and frequency of elongated mitochondria constrictions is higher in fibers from exercise-fatigued mice. The large majority of mitochondria in cross sectional areas of IIB/IIX fibers appear as thin elongated cylinders, oriented with their long axis in the transverse plane and located at the level of the I band where they form two branched networks that surround the myofibrils on either side of the Z line (Fig. 2). As in other mammalian muscles continuities within the network are quite extensive (Franzini-Armstrong, 2007), but it is also clear that frequent interruptions are present.

The average size of mitochondria profiles differs between resting and exercised muscles, resulting in thinner profiles in the latter although the same overall disposition is maintained (Fig. 2 A, B). The effect is quite noticeable by eye and it affects the entire mitochondria network in all type IIB/IIX fibers examined. A quantitative estimate of the effect was obtained by measuring the width of mitochondria profiles at a number of sites in a series of randomly collected images. The average mitochondria width is significantly smaller in fatigued EDL than EDL at rest: 0.10 ± 0.02 µm (mean ± SD) *vs* 0.14 ± 0.02 µm (Fig. 2C).

A second, independent variation in exercised IIX/IIB muscle fibers is a significant increase in mitochondria profiles involving unique elongated mitochondrial constrictions (EMC) connecting two adjacent segments of the same mitochondrion (Fig. 3A-F). These constrictions are suggestive of intermediate steps in fission process and are characterized by variable lengths, width and structure. Some EMC are constituted of a tubular formation containing visible matrix and cristae (Fig. 3A-C); others are considerably narrower and are delimited by a double mitochondrial membrane and characterized by an empty or totally collapsed lumen (Fig. 3D-F). The overall occurrence of EMCs is quite low. The frequency of mitochondrial constrictions in the entire cross sections of random IIX/IIB fibers in resting muscle is 0.65/fiber cross section (see methods). However, in fibers from exercised muscles, EMC, although still relatively rare, are significantly more frequent: 2.80/fiber cross section

(Fig 3G). This increase in EMC was present in all muscles from the exercised group (Fig. 3H). In order to determine the significance of these numbers, we obtained a rough count of the number of apparently individual mitochondrial profiles present in the same cross sections: 50/fiber cross section. This indicates that even in exercised muscle, only 5% of mitochondria were undergoing changes leading to constrictions at the time muscles were fixed, suggesting that the constrictions are rare and/or of short duration.

If EMC are indicative of an intermediate step in mitochondria fission, then some evidence should be found for successive stages. This indeed is the case: many of the elongated constriction sites evolve into very thin connecting necks (Fig. 3D-F). We call these structures “mitochondria on a string” (MOAS), as suggested by Zhang et al (2016) in the analysis of mitochondria in brain tissue. MOAS frequency is almost 40 times higher in fatigued versus resting fibers: 0.83 *vs* 0.022/ fiber (Fig. 2I). Comparison of figure 3G and 3I shows that about a third of the constrictions develop from the more variable shapes to the very thin ones. A final step is the actual fission of the mitochondrion into small fragments, with the loss of the extended elongated structures that characterize intermyofibrillar mitochondria in type IIB/IIX fibers. Exercised fibers show very little direct evidence for mitochondrial fragmentation, so constrictions do not necessarily lead to fission.

Overall mitochondria diameter decreases and frequency of Elongated Mitochondria Constrictions increases in electrically stimulated muscle. Fast twitch fibers in electrically stimulated EDL show slightly but significantly thinner mitochondria compared to unstimulated EDL with measured widths of 0.11 ± 0.02 (160 mitochondria, 15 cells, 3 mice) *vs* 0.14 ± 0.03 μm (146 mitochondria, 15 cells, 3 mice; mean ± SD, t-test, $p<0.0001$). Stimulated EDL fibers also display a significant increase in frequency of mitochondrial constrictions (Fig. 4A, E) involving the same variety of changes from partial to intense constrictions as observed in exercised fibers (compare with Fig. 3A, F). The frequency of elongated mitochondria constrictions in the stimulated *vs* resting EDL is 2.1 *vs* 0.94/fiber in cross section (Fig. 4F). The frequencies are essentially similar to those observed in muscles after exercises (see

section above and Fig. 3G). However there is not a significant incidence of the extreme case of multiple constrictions creating “mitochondria on a string” effect. In stimulated muscles small mitochondria clusters and mitochondria with a round rather than elongated profile are observed, suggesting an ongoing process of fragmentation (Fig. 4D, E). However, this effect is not frequent and, as indicated above, this is not obvious in muscles after exercise.

Drp1 recruitment to mitochondria membrane is affected by exercise and electrical stimulation. To investigate the molecular mechanism behind the formation of elongated mitochondria constrictions, we evaluated the expression and phosphorylation of a key fission protein: Dynamin Related Protein 1 (Drp1), in exercised muscle and electrically stimulated muscles. Phosphorylated Drp1 at Serine position 616 (Ser 616) promotes Drp1 translocation to the mitochondria, facilitating mitochondrial fission (Taguchi et al 2007). Levels of P-DRP1 (Ser616) are increased in EDL after treadmill exercise (Fig. 5A). The ratio P-DRP1 S616/Total DRP1 pixel density is increased by approximately 8 fold: 0.071 at rest *vs* 0.60 (Fig. 5B) suggesting an increase recruitment of DRP1 to mitochondria membrane. TA muscles after electrical stimulation show a slightly more modest ~4 fold increase inP-Drp1 (Ser616)/ Drp1: 4.18 *vs* 0.98 (Fig. 5D).

Levels of Drp1 total is slightly, but not significantly, increased in muscles after exercise but not after electrical stimulation. This situation can be explained as follows: the two experiments, physical exercise and electrical stimulation, involved different physiological conditions. To prepare mice to run on treadmill, they are first acclimated for one week and then subjected to run for up to one hour, the other mice were not prepared. Additionally the electrical stimulation is over a shorter period of 30 minutes and it involves less overall energy consumption and thus less possible anoxia than exercise.

Possible involvement of sarcoplasmic reticulum in the development of mitochondria constrictions. We observe a specific, potentially significant interaction between SR and mitochondria at sites of constrictions: SR fingers are very frequently closely opposed to constricted sites and seem to push into them (Fig. 6). A wedge may appear to be inserted in the elongated neck region (Fig. 6A-C), or an elongated finger closely encircles a constricted

mitochondrial segment forming a ring around it (Fig. 6 G-J). In the area of contact between the SR and mitochondria membrane electron dense areas are seen (Fig. 6 D-F). SR closely opposed to the EMCs is observed in all conditions at a frequency (SR closely associated/EMCs x 100) of: 16% in resting, 31% in run, 26% in control and 28% in stimulated muscles.

Discussion

Our imaging data show that acute exercise and electrical muscle stimulation induce an increase in intermediate and advanced stages of mitochondria stress dependent events possibly leading to fission in fast/fatigable fibers. The noticeable effect is the formation of unusual mitochondrial profiles with elongated constrictions (EMCs) that constitute a novel direct view of the process. Constrictions are quite rare in resting muscle and thus had so far escaped attention and obviously have been missed in past studies of fatigued muscle. Most of the constrictions that we observe are of short length and they may be of brief duration in line with mitochondria's highly dynamic responses. However, it is conceivable that if similar constrictions are long lived, they may develop into the very thin elongated connections between mitochondria observed in brain tissue of mice carrying human FAD (familial Alzehimer's disease) mutations (Zhang et al., 2016), and in some not well-defined conditions of human pathology (Vincent et al., 2016).

If mitochondria undergo fission, the obvious question is whether this fission results in the appearance of small mitochondria profiles deriving from fragmentation of the normal elongated mitochondria. Mitochondria fragmentation, resulting in accumulation of smaller organelles, is easily detected in conditions of energetic stress and unbalanced Ca^{2+} homeostasis (Wu et al., 2010, Iqbal and Hood, 2015; Lavorato et al., 2015). However, despite evidence for possible mitochondria fission events, we find very little obvious evidence for fragmented mitochondria after electrical stimulation and practically no evidence after treadmill exercise. This may be in part due to the fact that only a minor portion (~5%) of the mitochondria show evidence for actual fission at one time. Gollnick and King (1969) have shown an apparent increase in the frequency of mitochondrial profiles in exercised rat

muscle, but have not demonstrated any direct evidence for their origin. More importantly, either the fission process in fatigued muscles is slow, or the increase in DRP1 may be related more to activation of respiration (Wei et al., 2011; Zhang et al., 2017) than to actual fission. It is reassuring that fatigue induced under functional conditions not different from that encountered by humans performing endurance exercise (primarily an oxygen-dependent form of exercise such as long distance running) has a definite effect on mitochondria but does not result in massive fragmentation.

Considering that Drp1 activation via S616 phosphorylation (Taguchi et al., 2007) is related to mitochondrial fission and that S616 phosphorylation is observed in muscle affected by acute exercise or stimulation, it is likely that the observed increase in EMC is due to an increase in Drp1 recruitment to mitochondria membrane that induces incipient fission. However, the process of fission is apparently somewhat slowed down or arrested in intermediate stages. Indeed, increase in mitochondria constrictions frequency is associated with increased level of P-DRP1 (S616) and with a delay in fission process in an Alzheimer disease model (Zhang et al., 2015).

Several factors may explain the small differences observed between fatigue induced by extensive exercise and by direct muscle stimulation. First, the duration of the electrical stimulation protocol was shorter: 30 *vs* 45-60 minutes. Secondly, oxygen consumption and thus hypoxia must be considerably less in the electrical stimulation, which involves only the leg muscles, while most of the body muscles are involved during physical exercise. Thus low oxygen stress may be a contributing factor in the stimulation of mitochondrial fission. Additionally, mice subjected to treadmill exercise were acclimated for one week; this may affect mitochondrial biogenesis and synthesis of mitochondrial proteins such as Drp1, increasing its levels at rest and affecting its response to the running exercise stimulus.

Using both 2D and 3D microscopy we observed that the sarcoplasmic reticulum may be closely opposed to the sites where mitochondria are thinned and extended (EMC) in a manner highly suggestive of a role in inducing constrictions. A role for ER in initiating mitochondrial fission has been proposed on the basis of light microscope observations

(Friedman et al., 2011) but not demonstrated at higher resolution. We clearly detect the formation of SR wedges at sites of incipient mitochondrial constrictions thus providing a new insight into the relationship between SR and mitochondria in the fission process. The SR may facilitate the sharp change in membrane curvature that occurs at sites of EMCs.

It is not clear how the small but significant decrease in mitochondria volume detected as a small change in their diameter is related to the constriction events. Since the latter are fairly rare while the former affects the entire network, the two may not be related.

Acknowkledgements

We thank Dr. Stephen Hollingworth for constructive suggestions. Supported by National Institute of Arthritis and Musculoskeletal and Skin Diseases (NIAMS) grant AR 052354-06A1, PI: P. D. Allen (to C.F-A.).

References

Abrams, A.J., Hufnagel R.B., Rebelo, A., Zanna, C., Patel, N., Gonzalez, M. A., Campeanu, I. J., Griffin L. B., Groenewald S., Strickland, A.V., Tao, F., Speziani, F., et al. (2015). Mutations in the UGO1-like protein SLC25A46 cause an opticatrophy spectrum disorder. *Nat. Genet.* **47**, 926–932.

Allen DG, Westerblad H., Lännergren J. (1992). Role of excitation-contraction coupling in muscle fatigue. *Sports Med* 13(2):116-26, 1992 .Allen DG, Westerblad H (2001) Role of phosphate and calcium stores in muscle fatigue. *J. Physiol.* **536** (Pt3): 657-65.

Bangsbo J. (2000). Muscle oxygen uptake in humans at onset of and during intense exercise. *Acta. Physiol. Scand.* **168**:457-64.

Boncompagni S, Rossi A.E., Micaroni M., Beznoussenko G.V., Polishchuk R.S., Dirksen R.T., Protasi F. (2009a). Mitochondria are linked to calcium stores in striated muscle by developmentally regulated tethering structures. *Mol. Biol. Cell.* **20** (3):1058-67.

Boncompagni S., Rossi A.E., Micaroni M., Hamilton S.L., Dirksen R.T., Franzini-Armstrong C., Protasi F. (2009b). Characterization and temporal development of cores in a mouse model of malignant hyperthermia. *Proc. Natl. Acad. Sci. USA.* **106**(51):21996-2001.

Bruton J., Jeffries G.D., Westerblad H. (2014). Usage of a localised microflow device to show that mitochondrial networks are not extensive in skeletal muscle fibres. *PLoS ONE.* **9**(9):e108601.

Chan D.C. (2012). Fusion and Fission: Interlinked Processes Critical for Mitochondrial Health. *Annu. Rev. Genet.* **46**:265–87.

Chen H., Chan D.C. (2010). Physiological functions of mitochondrial fusion. *Ann. NY Acad. Sci*.**1201**: 21–25.

Cheng AJ, Yamada T., Rassier D.E., Andersson D.C., Westerblad H., Lanner J.T. (2016) Reactive oxygen/nitrogen species and contractile function in skeletal muscle during fatigue and recovery. *J Physiol* **594**(18):5149-60. ‘

Coronado M., Fajardo G., Nguyen K., Zhao M., Kooiker K., Jung G., Hu D-K., Reddy S., Stotland A., Gottlieb R.A., Bernstein D. (2018). Physiological Mitochondrial Fragmentation Is a Normal Cardiac Adaptation to Increased Energy Demand. *Circ. Res.* **122**: 282-295

Dahl R, Larswen S, Dohlman TL, Helge JW, Dela F and Prats C. (2015). Three-dimensional reconstruction of the human skeletal muscle mitochondrial network as a tool to assess mitochondrial content and structural organization. *Acta Physiol (Oxf)* 213, 145–155.

Danieli-Betto D., Esposito A., Germinario E., Sandonà D., Martinello T., Jakubiec-Puka A., Biral D., Betto R. (2005) Deficiency of alpha-sarco-glycan differently affects fast- and slow-twitch skeletal muscles. *Am. J. Physiol. Regul. Integr. Comp. Physiol.* **289**, R1328–R1337.

Detmer S.A., Chan D.C. (2007). Functions and dysfunctions of mitochondrial dynamics. *Nat. Rev. Mol. Cell. Biol.* **8**:870–9.

Dirksen R.T. (2009). Sarcoplasmic Reticulum-Mitochondrial "Through-Space" Coupling in Skeletal Muscle. *Appl. Physiol. Nutr. Metab.* **34**(3):389-95.

Franzini-Armstrong C. (2007). ER-Mitochondria Communication. How Privileged? Physiology (Bethesda). **22**:261-268.

Franzini-Armstrong C., Boncompagni,S. (2011). The Evolution of the Mitochondria-to-Calcium Release Units Relationship in Vertebrate Skeletal Muscles," J. Biomed. Biotech, **2011**:830573.

Friedman J.R., Lackner L.L., West M., DiBenedetto J.R., Nunnari J., Voeltz G.K. (2011). ER Tubules Mark Sites of Mitochondrial Division. *Science.* **334**:358-362.

Fitt. R.H. (1994). Cellular mechanisms of muscle fatigue. *Physiol. Rev.* **74**:49-94.

Glancy B., Hartnell L.M., Malide D., Yu Z.X., Combs C.A., Connelly P.S., Subramaniam S., Balaban R.S. (2015) Mitochondrial reticulum for cellular energy distribution in muscle. *Nature.* **523**:617–620.

Gollnick P.D., King D.W. (1969). Effect of exercise and training on mitochondria of rat skeletal muscle. *Am. J. Physiol.* **216**:1502-1509.

Hoffman N.J., Parker B.L., Chaudhuri R., Fisher-Wellman K.H., Kleinert M., Humphrey S.J., Yang P., Holliday M., Trefely S., Fazakerley D.J., et al. (2015) Global Phosphoproteomic Analysis of Human Skeletal Muscle Reveals a Network of Exercise-Regulated Kinases and AMPK Substrates. *Cell. Metab.* **22**(5):922–935.

Hughes S.M., Chi M.M., Lowry O.H., Gundersen K. (1999). Myogenin induces a shift of enzyme activity from glycolytic to oxidative meta- bolism in muscles of transgenic mice. *J. Cell. Biol.* **145**(3):633–642.

Iqbal S., Hood D.A. (2014). Oxidative stress-induced mitochondrial fragmentation and movement in skeletal muscle myoblasts. *Am. J. Physiol. Cell Physiol.* **306**(12):C1176-83.

Kamandulis S., de Souza Leite F., Hernández A., Katz A., Brazaitis M., Bruton J.D., Venckunas T., Masiulis N., Mickeviciene D., Eimantas N., et al. (2017) Prolonged force depression after mechanically demanding contractions is largely independent of Ca^{2+} and reactive oxygen species. *ASEB J.* **31**(11):4809-4820.

Kata A., Andersson D.C., Yu J., Norman B., Sandstrom M.E., Wieringa B., Westerblad H. (2003). Contraction-mediated glycogenolysis in mouse skeletal muscle lacking creatine kinase: the role of phosphorylase b activation. *J. Physiol.* **555**(2):523-531.

Lavorato M., Gupta P.K., Hopkins P.M., Franzini-Armstrong C. (2016). Skeletal muscle microalterations in patients carrying Malignant Hyperthermia-related mutations of the e-c coupling machinery. *Eur. J. Transl. Myol.* **26**: 6105.

Lavorato M., Huang T.Q., Iyer V.R., Perni S., Meissner G., Franzini-Armstrong C. (2015). Dyad content is reduced in cardiac myocytes of mice with impaired calmodulin regulation of RyR2. *J. Muscle Res. Cell. Motil.* **36**(2): 205-14.

Lavorato M, Iyer V.R., Dewight W., Cupo R.R., Debattisti V., Gomez L., De la Fuente S., Zhao Y.T., Valdivia H.H., Hajnóczky G., Franzini-Armstrong C. (2017). Increased mitochondrial nanotunneling activity, induced by calcium imbalance, affects intermitochondrial matrix exchanges. *Proc. Natl. Acad. Sci. USA.* **114**(5):E849–E858.

Loro E, Seifert E.L., Moffat C., Romero F., Mishra M.K., Sun Z., Krajacic P., Anokye-Danso F., Summer R.S., Ahima R.S., Khurana T.S. (2015) IL-15Rα is a determinant of muscle fuel utilization, and its loss protects against obesity. *Am. J. Physiol. Regul. Integr. Comp. Physiol.* **309**(8):R835–44.

Mannella C.A., Buttle K., Rath B.H., Marko M. (1998). Electron microscopic tomography of rat-liver mitochondria and their interaction with the endoplasmic reticulum. *Biofactors.* **8**:225-228.

Nagasser A.S., van der Laarse W.E., Elzinga G. (1992). Metabolic changes with fatigue in different types of single musckle fibers of Xenopus laevis. *J. Physiol.* **448**:511-523.

Nassar-Gentina V., Passonneau J.V., Rapoport S.I. (1981). Fatigue and metabolism of frog muscle fibers during stimulation and in response to caffeine. *Am. J. Physiol.* **241**(3):C160-6.

Ogata T., Yamasaki Y. (1990): High-resolution scanning electron microscopic studies on the three-dimensional structure of the transverse-axial tubular system, sarcoplasmic reticulum and intercalated disc of the rat myocardium. *Anat. Rec.* **228**: 277–287.

Ogata T., Yamasaki, Y. (1993). Ultra-high resolution scanning electron microscopic studies on the sarcoplasmic reticulum and mitochondria in various muscles: a review.*Scan. Microsc.* **7**:145–156.

Picard M., Gentil B.J., McManus M.J., White K., St Louis K., Gartside S.E., Wallace D.C., Turnbull D.M. (2013) Acute exercise remodels mitochondrial membrane interactions in mouse skeletal muscle. *J. Appl. Physiol.* **115**(10): 1562–1571.

Potts G.K., McNally R.M., Blanco R., You J.S., Hebert A.S., Westphall M.S., Coon J.J., Hornberger T.A. (2017). A map of the phosphoproteomic alterations that occur after a bout of maximal-intensity contractions. *J. Physiol.* **595**: 5209–5226.

Rana A., Oliveira M.P.,. Khamoui A.V., Aparicio R., Rera M., Rossiter H.B., Walker DW. (2017). Promoting Drp1-mediated mitochondrial fission in midlife prolongs healthy lifespan of Drosophila melanogaster. *Nature Comm*. **8**: 448-451.

Rossi E., Boncompagni E., Dirksen R.T. (2009). Sarcoplasmic reticulum-mitochondrial symbiosis: bidirectional signaling in skeletal muscle. *Exerc. Sport Sci. Rev.* **37**: 29–35.

Tinel H., Cancela J.M., Mogami H., Gerasimenko J.V., Gerasimenko O.V., Tepikin A.V., Petersen O.H. (1999). Active mitochondria surrounding the pancreatic acinar granule region prevent spreading of inositol trisphosphate-evoked local cytosolic Ca ($^{2+}$) signals. *EMBO J.* **18**:4999-5008.

Tanaka K., Mitsushima A. (1984). A preparation method for observing intracellular structures by scanning electron microscopy. *J. Microsc.* **133**:213–222.

Taguchi N., Ishihara N., Jofuku A., Oka T., Mihara K. (2007). Mitotic phosphorylation of dynamin-related GTPase Drp1 participates in mitochondrial fission. *J. Biol. Chem.* **282**:11521–11529.

Vincent A.E., Ng Y.S., White K., Davey T., Mannella C., Falkous G., Feeney C., Schaefer A.M, McFarland R., Gorman G.S., et al. (2016). The spectrum of mitochondrial ultrastructural defects in mitochondrial myopathy. *Sci. Rep.* **6**:30610-30622.

Wei L., Slahura G., Boncompagni S., Kasischke K.A., Protasi F., Sheu S.S., Dirksen R.T. (2011). Mitochondrial superoxide flashes: metabolic biomarkers of skeletal muscle activity and disease. *FASEB J.* **25**:3068-3078.

Westerblad H., Allen D.G. (1992). Myoplasmic free Mg^{2+} concentration during repetitive stimulation of single fibres from mouse skeletal muscle. *J. Physiol.* **453**:413-34.

Westerblad H.; Allen D.G. (1993). The influence of intracellular pH on contraction, relaxation and $[Ca^{2+}]i$ in intact single fibres from mouse muscle. *J. Physiol.* **466**:611-28.

Westermann B. (2010) Mitochondrial fusion and fission in cell life and death. *Nat. Rev. Mol. Cel.l Biol.* **11**: 872–884.

Wu S., Zhou F., Zhang Z., Xing D. (2010). Mitochondrial oxidative stress causes mitochondrial fragmentation via differential modulation of mitochondrial fission–fusion proteins. *FEBS J.* **278**:941-54.

Zhang H., Wang P., Bisetto S., Yoon Y., Chen Q., Sheu S.S., Wang W. (2017). A novel fission-independent role of dynamin-related protein 1 in cardiac mitochondrial respiration. Cardiovasc. Res. **113**:160-170.

Zhang L., Trushin S., Christensen T.A., Bachmeier B.V., Gateno B., Schroeder A., Yao J., Itoh K., Sesaki H., Poon W.W., et al. (2016) Altered brain energetics induces mitochondrial fission arrest in Alzheimer's Disease. *Sci Rep.* **5**:18725.

Figures

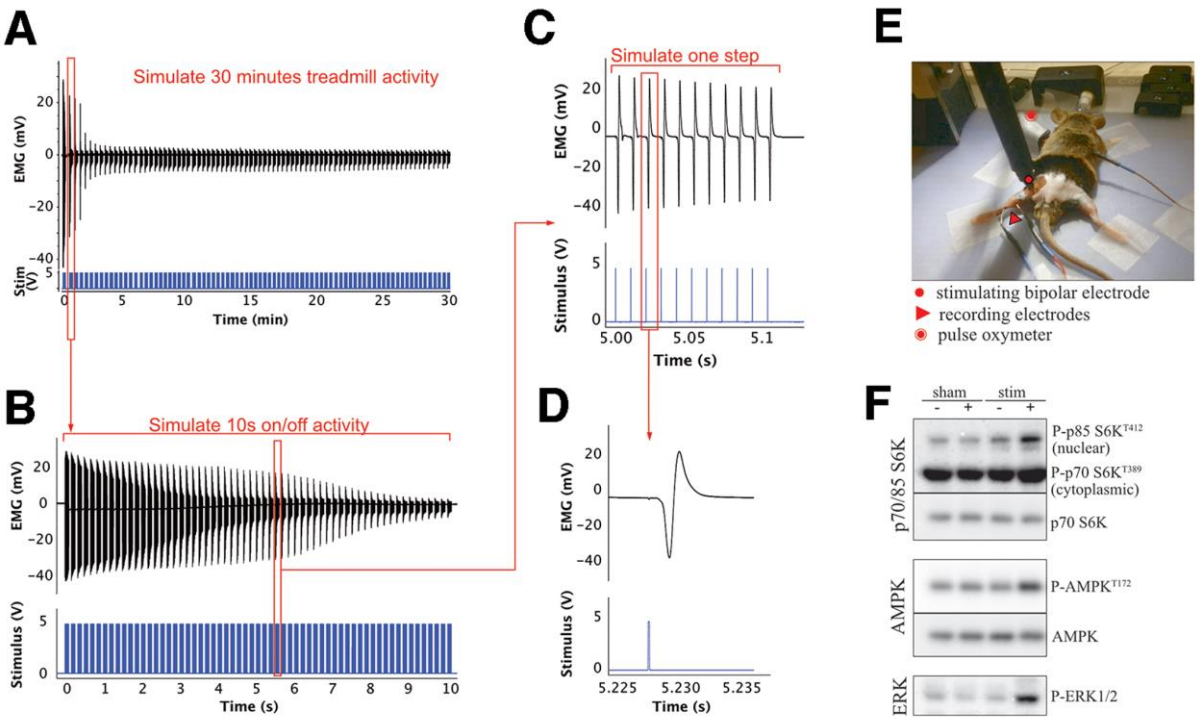

Figure 1. Sciatic nerve high-intensity stimulation protocol. A, B) Electromyographic (EMG) and stimulus traces over 30 minutes of intermittent (10s ON/ 10s OFF) sciatic stimulation that mimics the mouse frequently interrupted running activity (see methods) A) Each stimulus trace (in blue) represents a burst of 10 sec, and it is shown in detail in B. The EMG amplitude, relating the muscle response, shows ~ 80% decrease in amplitude within the first 5 minutes and a small decline after that. B) A detail of a single burst of 5V stimuli at 100 Hz repeated at 6/sec. It shows the response's decline within one of the initial bursts. C) Enlarged representation of a few of the evoked muscle action potentials repeated at 100Hz for 100ms in each burst. D) Single muscle action potential evoked stimulating the sciatic nerve with a 5V stimulus. E) Stimulating and recording electrodes placement. F) Stimulation-induces increased phosphorylation of known exercise-sensitive proteins such as p70/85S6K, AMPK.

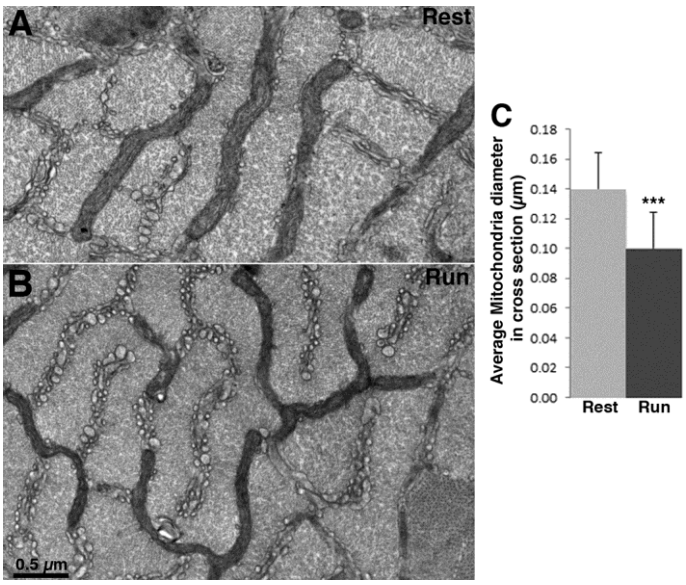

Figure 2. Mitochondria are smaller in fast twitch fibers of mice at the end of a run. A, B) Cross section of IIX/B fibers at the level of the I band in EDL at rest and after mice run on a treadmill to the point of exhaustion. Mitochondria are located between myofibrils in two transverse planes on either side of the Z line. Mitochondria have the same overall distribution, but they are noticeably thinner in fibers of mice after treadmill exercise (B) than in fibers of mice at rest (A). C) The average mitochondria width measured at 2/3 spots for each mitochondrion at right angle to the long axis of the organelle is 0.10 ± 0.02 µm in fibers from exercised mice (Run) (mean ± SD, n=251 mitochondria, 20 cells, 41 images at 26300x, 4 mice) and 0.14 ± 0.02 µm in fibers from resting mice (Rest) (n=190 mitochondria, 23 cells, 40 areas at 26300x, 4 mice); student's t-test*** $p<0.0001$.

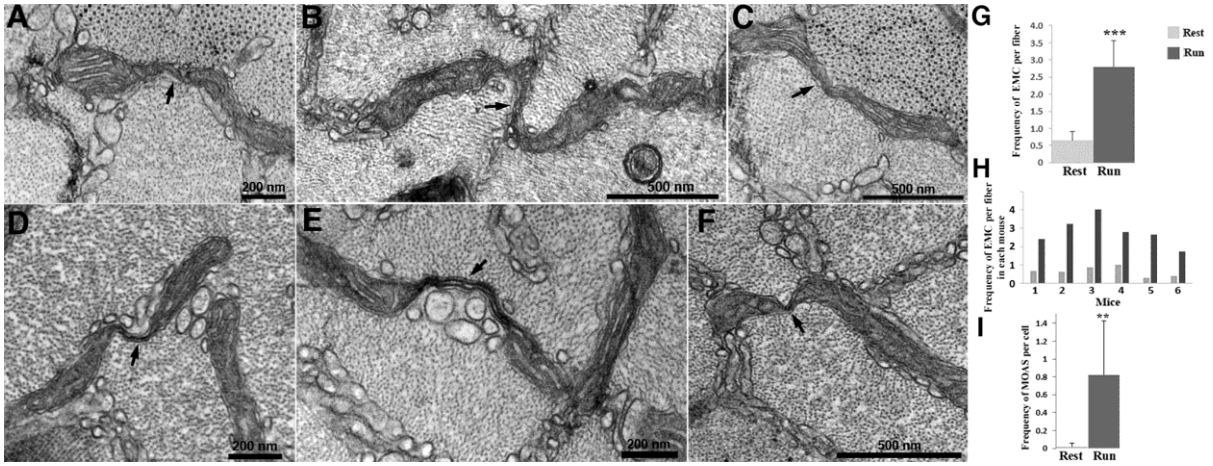

Figure 3. Elongated Mitochondrial Constrictions (EMC) in fast twitch fibers after fatigue. A close examination of the elongated mitochondria within the I band reveals sites at which the width of the organelle is abruptly decreased resulting in a narrow neck (arrows) connecting two adjacent sections of the same mitochondrion. The extent and size of elongated constrictions are quite variable and their frequency depends on the muscle status, resting versus fatigued. All images shown are from fatigued muscles. A-C) Intermediate stages where the matrix and cristae are visible in the constricted region. D-F) Extreme cases of elongated constriction most likely the last stage of the fission process, where the very thin neck is composed only of the double mitochondrial membrane. Mitochondria connected by these extreme constrictions are called MOAS (mitochondria on a string, by Zhang et al, 2016). G). EMC frequency/fiber is significantly higher in mice after a run compared to mice at rest: 2.80 ± 0.77 (n=6 mice, 53 fibers) *vs* 0.65 ± 0.27 (n=6 mice, 58 fibers); ***p< 0.001. H) Frequency of EMC in fibers from individual mice at rest and after running. I) MOAS (mitochondria on a string) frequency is significantly higher in EDL after a run then in EDL at rest: 0.83 ± 0.60 (n=6 mice, 53 fibers) *vs* 0.02 ± 0.04, **p<0.01 (n=6 mice, 58 fibers).

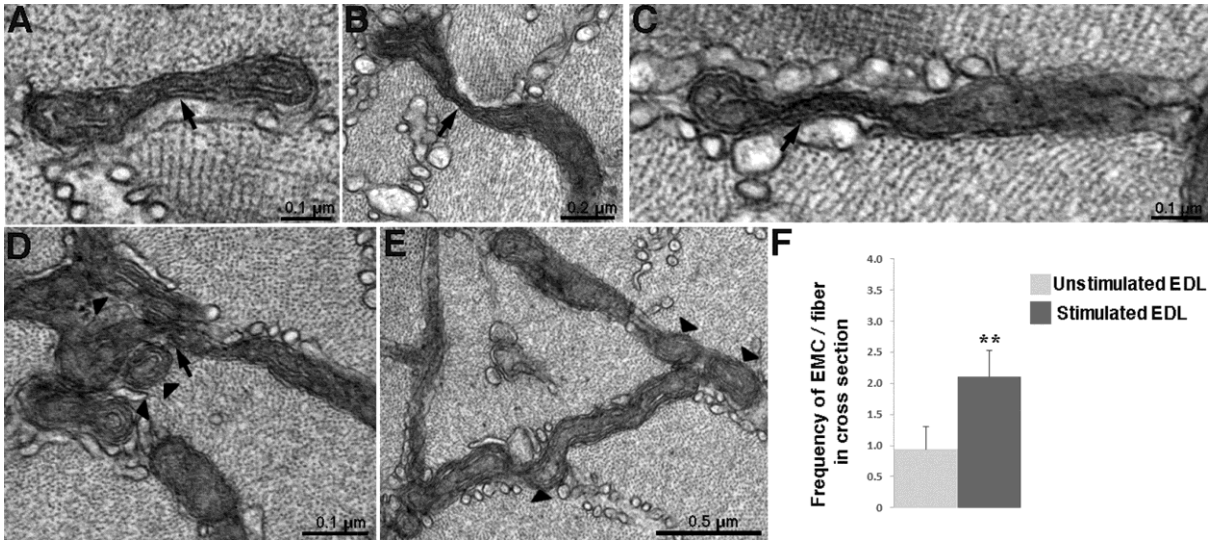

Figure 4. Elongated mitochondria constrictions in fatigue induced by electrical stimulation. A-C. Cross sections of fibers from electrically stimulated muscles demonstrate the presence of elongated mitochondria constrictions (arrows). F) The frequency of Elongated Mitochondria Constrictions (EMC) is significantly higher in electrically stimulated EDLs than in the unstimulated ones: 2.10 ± 0.42/fiber (n= 45 fibers, 4 mice,) *vs* 0.94 ± 0.36 (n= 42 fibers, 4 mice,); **p< 0.01. D) The presence of EMC (arrows) is sometimes accompanied by clusters of rounded small mitochondrial profiles (arrowheads) which may originate from fission events. E) Round profiles appearing at the end of mitochondria are indicative of fragmentation (arrowhead).

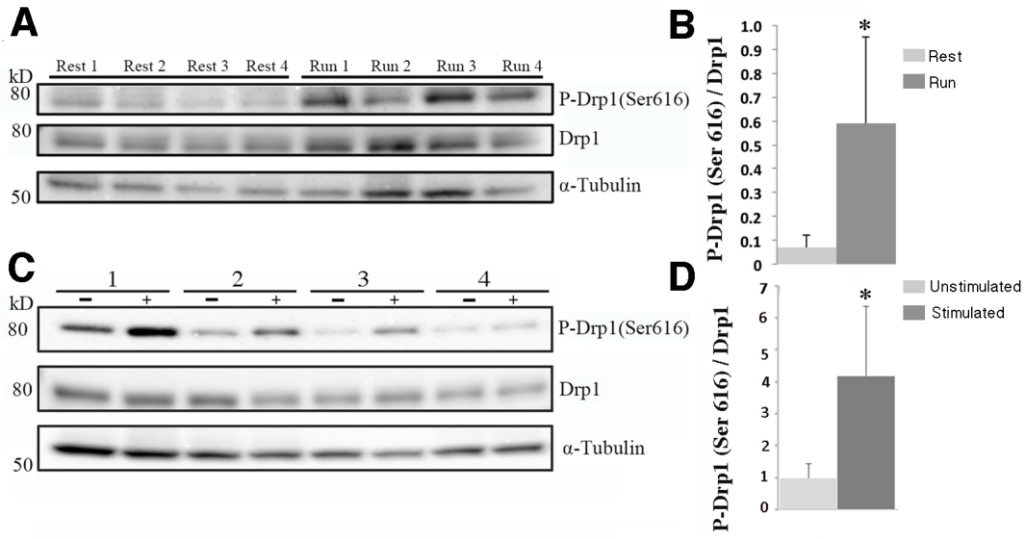

Figure 5. Increases P-DRP1 (Ser616) levels in mitochondria of exercised and electrically stimulated muscles. A, C) Immunoblot of P-DRP1 S616 and DRP1 total in mouse EDL at rest and after running (n=4 mice each) and TA in unstimulated at electrically stimulated (n=4 mice each). In C, 1-4 indicate the number mice used. B) The pixel density ratio P-DRP1 S616/Total DRP1 is 8-fold higher in EDL after exercise compared to the resting muscles (0.071±0.05 vs 0.60±0.36, paired t-test $p<0.05$). D) DRP1 S616 phosphorylation is 4.3-fold higher in stimulated TA than in unstimulated TA (4.18 ± 4.35 vs 0.98 C 0.93; *$p<0.05$; paired t-test). The densitometric ratio of S616 tubulin is also higher in run versus control (0.005±0.003 vs 0.0008±0.0008 mean ± SD *$p<0.05$; paired t-test) and in stimulated versus contralateral leg (1.31±1.77 versus 0.42±0.30 $p=0.09$).

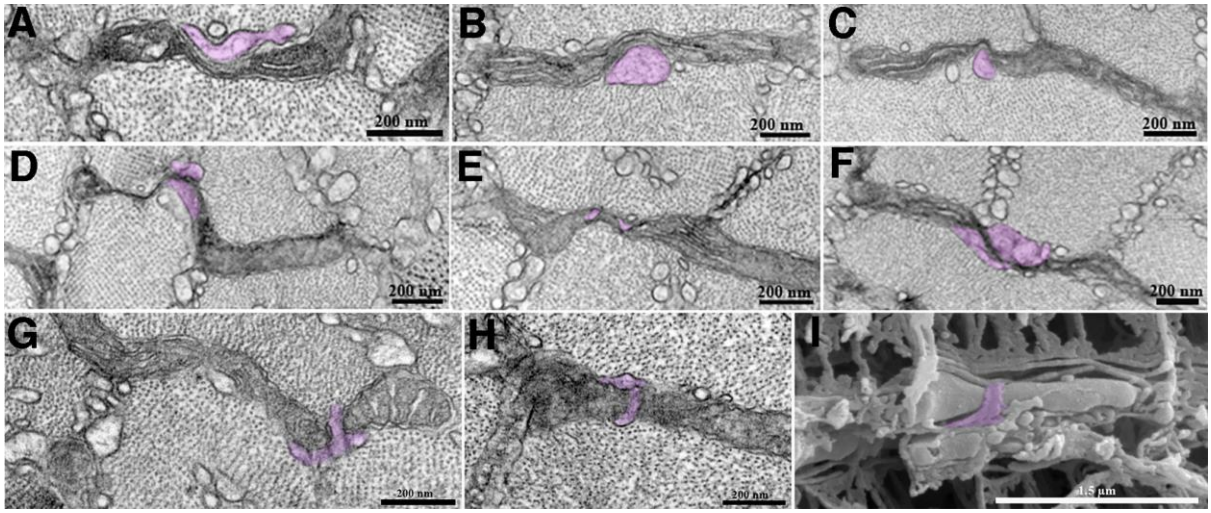

Figure 6. Mitochondria constrictions and Sarcoplasmic Reticulum (SR). SR (in purple) is often very closely associated with mitochondria constrictions either forming a sort of wedge (A-C) or wrapping around mitochondria especially around the neck of the organelle at sites of constriction (D, H). These structures were also observed by three-dimensional scanning electron microscopy (I).

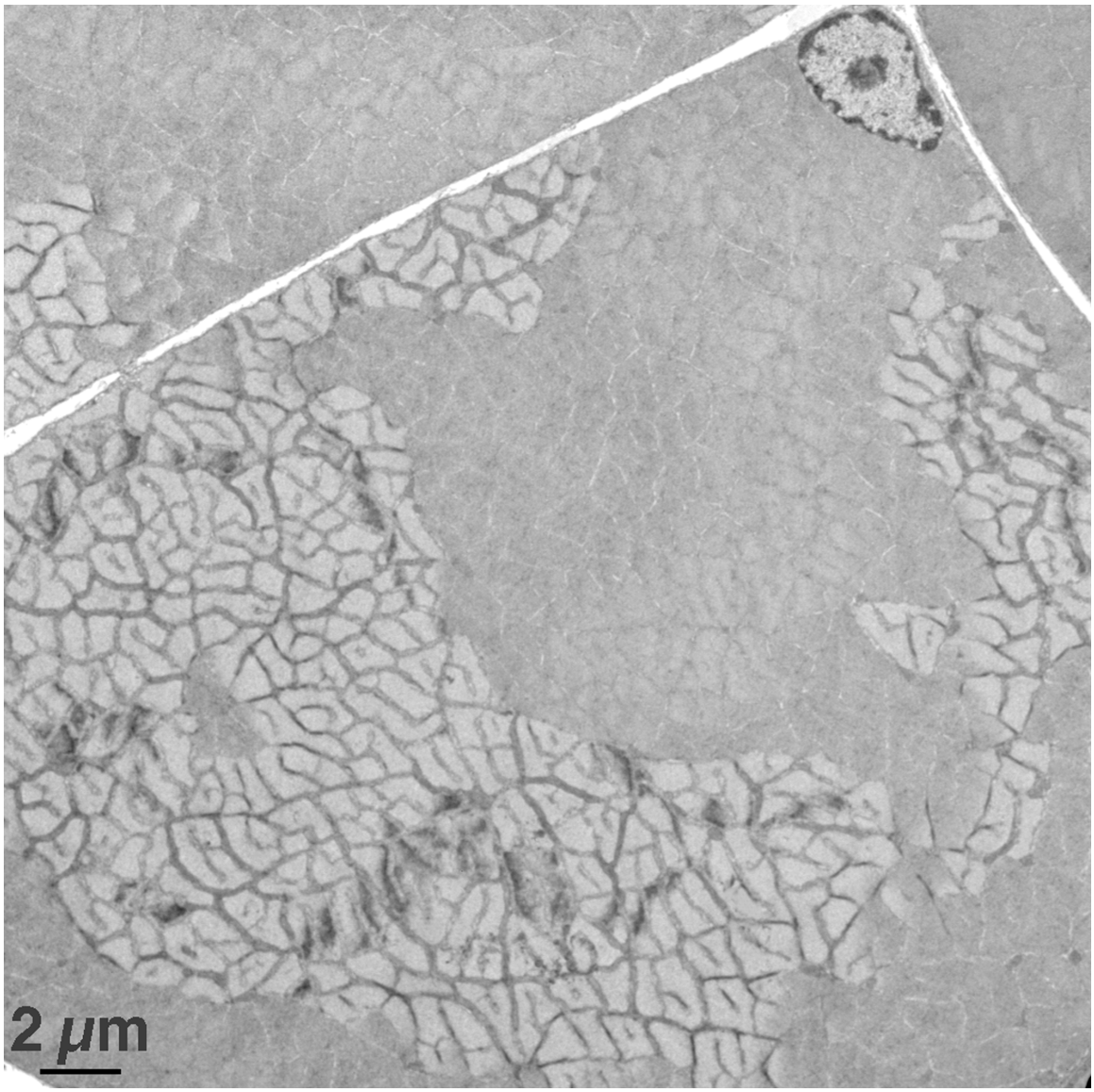

Figure S1. Low magnification image illustrating the standard quality of preservation and orientation of the images that were used to collect the data. Each cross sectional view had excellent presentations of I- and A- band areas and only images that covered entire fiber cross sections were employed for counts. The I-band areas were used for obtaining counts of the frequency of mitochondria with constrictions of the type illustrated in Figs. 3-5. A large sample (> 40 fibers each for rest and fatigued muscles) assured sufficient statistical reliability.

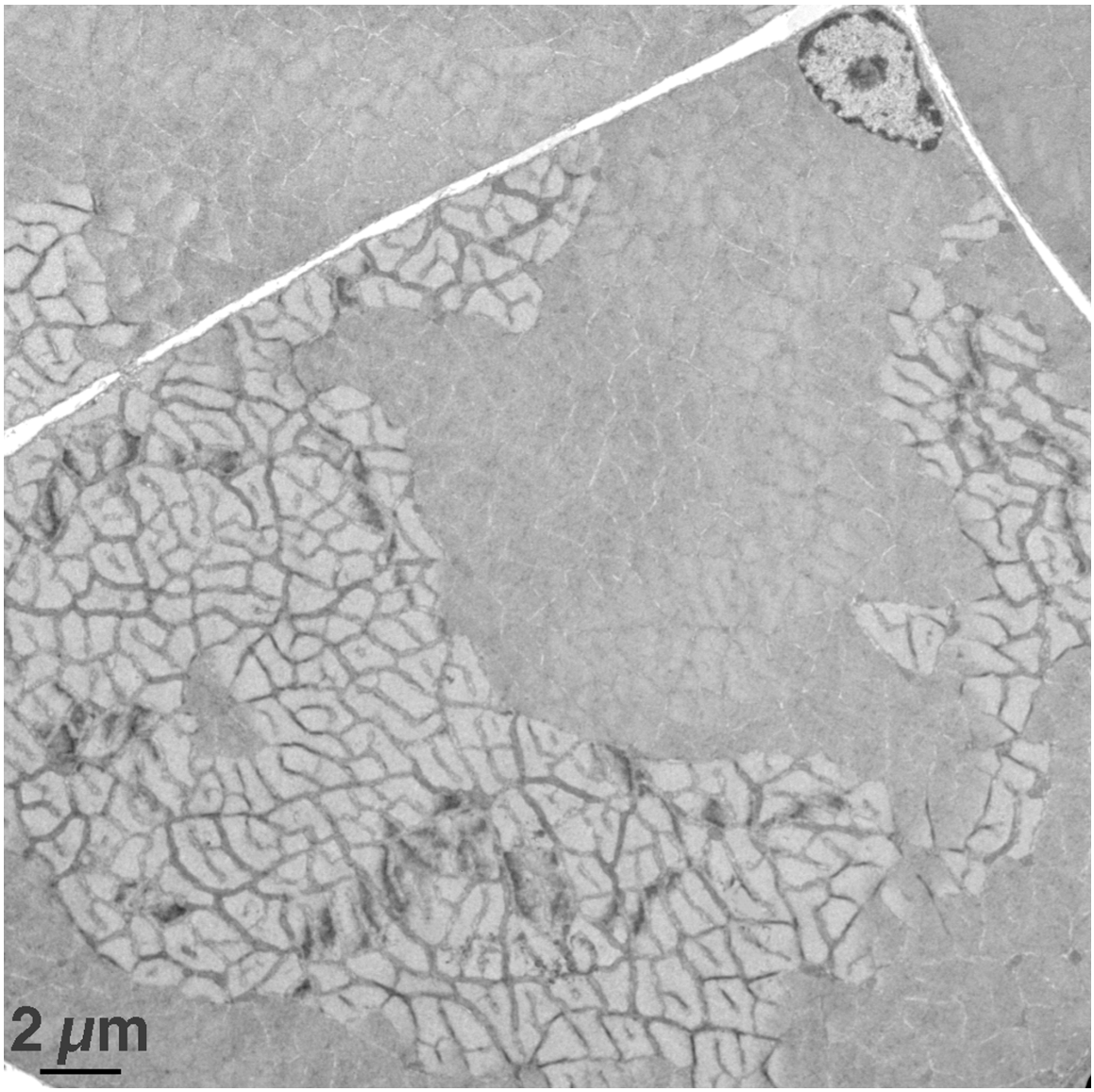

Figure S1. Low magnification image illustrating the standard quality of preservation and orientation of the images that were used to collect the data. Each cross sectional view had excellent presentations of I- and A- band areas and only images that covered entire fiber cross sections were employed for counts. The I-band areas were used for obtaining counts of the frequency of mitochondria with constrictions of the type illustrated in Figs. 2-4. A large sample (> 40 fibers each for rest and fatigued muscles) assured sufficient statistical reliability.